Complex Permittivity Evaluation of Building Materials at 200-500 GHz Using THz-TDS

Masaaki Urahashi, Ryo Okumura, Koji Suizu, and Akihiko Hirata
Chiba Institute of Technology
Faculty of Engineering
Narashino-shi, Chiba, Japan
hirata.akihiko@p.chibakoudai.jp

***Abstract*—In the next-generation mobile communication standard (5G), the use of terahertz (THz) waves in the 300-GHz band is a promising candidate for achieving ultra-high-speed wireless communication. In order to put the 300-GHz band wireless link into practical use, it is necessary to construct a propagation model in these bands, however, the experimental data on the reflectance and transmittance of building materials in the 300GHz band was insufficient to construct a propagation model.**

In this paper, we employed terahertz time-domain spectroscopy (THz-TDS) spectroscopy to obtain the complex permittivity of building materials, glass, concrete, and granite at 200-500 GHz, in order to calculate the reflectance and transmittance of building materials. In THz-TDS spectroscopy measurement, the effect of multiple reflections was removed by time-gating the acquired waveform. We conducted 300-GHz-band indoor radio wave propagation simulation by using the calculated complex permittivity of building materials.

Keywords—Terahertz, THz-TDS, complex permittivity

I. INTRODUCTION

In recent years, mobile traffic has rapidly increased due to the spread of smart phones and tablets. In order to catch up with the rapid increase in mobile traffic, services for 5G mobile communication systems have been started in 2019. 5G mobile communication is expected to be used in all areas, such as device control systems, IoT devices and management systems in addition to smartphones. In order to respond to the further increase in mobile traffic, research and development of next-generation mobile communication standard, beyond 5G, has started. Beyond 5G is considering the use of terahertz (THz) waves in the 300 GHz band to support ultra-high-speed communications [1]. In order to put the 300GHz-band wireless link into practical use, it is necessary to construct a propagation model in these bands for the sharing studies with other systems and for the prediction of communication quality of wireless systems. In the frequency bands below 60 GHz, the ITU-R recommendations have already specified the radio wave propagation model. However, the 300 GHz band is an unexplored frequency band, and only a few experiments on radio wave propagation have been conducted. Therefore, radio wave propagation model at 300 GHz band has not been constructed. In particular, there was only a few data on the reflectance or transmittance of building materials in the 300 GHz band.

In this paper, we employed terahertz time-domain spectroscopy (THz-TDS) to obtain the complex permittivity of building materials in order to calculate the reflectance and transmittance of building materials such as concrete and glass. THz-TDS is a spectroscopic technique in which the properties of materials are probed with short pulses of terahertz radiation. The generation and detection scheme is sensitive to the sample's effect on both the amplitude and the phase of the terahertz radiation. The complex permittivity of the sample can be calculated by injecting the s-polarized wave and p-polarized wave into the sample and calculating the ratio of the reflected signals. A vector network analyzer (VNA) can be used to calculate the complex permittivity of a sample in the similar way. However, it is difficult for VNA to eliminate the influence of multiple reflection signals with small delay time. Since the pulse width of THz-TDS is below 1 psec, multiple reflection can be eliminated by applying time-gating to the measured time waveform for a sample affected by the multiple reflection at the backside, such as glass of several mm thickness. In this paper, we measured the complex permittivity of these building materials, such as concrete, glass, and granite, at 200-500 GHz by THz-TDS. Furthermore, we simulated indoor 300-GHz band propagation by using the measured complex permittivity of the building material .

II. EXPERIMENTAL SETUP

THz-TDS is one of the methods of generating and detecting terahertz wave pulses [2], which enables us to make time-resolved measurements of electromagnetic waves. In general ellipsometry, an electromagnetic wave is obliquely incident on a material and the reflection intensity of s and p polarization is measured. The phase difference between the reflected p-polarized and s-polarized electromagnetic waves is measured by rotating a polarizer (wire grid), and the optical constant of the material is calculated from the phase difference.

An s-polarized and p-polarized electromagnetic (EM) wave with equal amplitude and phase is injected into a sample at an incidence angle θ. The complex permittivity is calculated from the ratio of reflectance to s-polarized and p-polarized EM waves as r_s and r_p, respectively. The following is diagram (Fig. 1) and photograph (Fig. 2) of the measurements and the formula for calculating the complex permittivity.

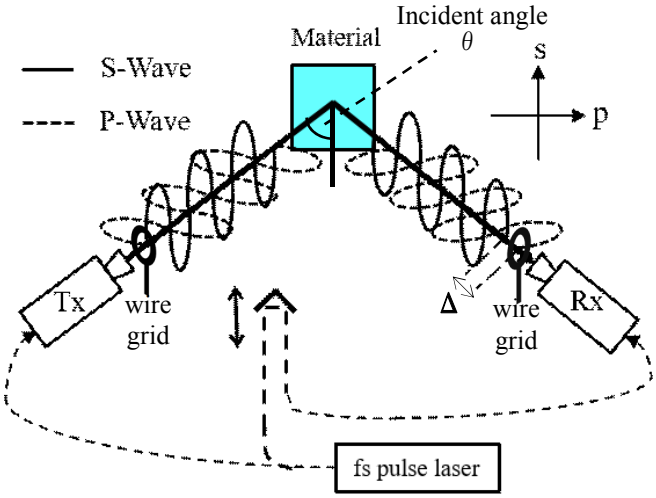

Fig. 1 Experimental setup of THz-TDS

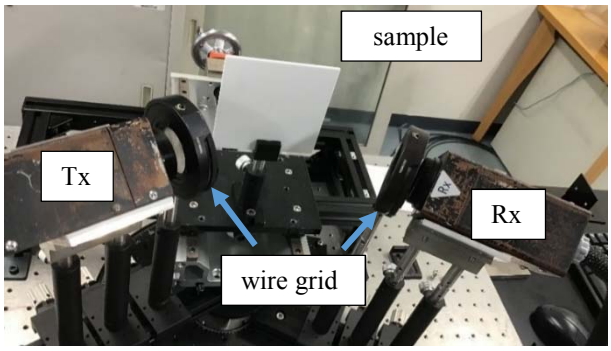

Fig. 2 Photograph experimental setup of THz-TDS

The measured r_s and r_p are defined in Eq. (1) and Eq. (2), respectively [3]

$$r_s = \frac{\cos\theta - \sqrt{n_2^2 - \sin^2\theta}}{\cos\theta + \sqrt{n_2^2 - \sin^2\theta}} \quad \cdots (1)$$

$$r_p = \frac{n_2^2\cos\theta - \sqrt{n_2^2 - \sin^2\theta}}{n_2^2\cos\theta + \sqrt{n_2^2 - \sin^2\theta}} \quad \cdots (2)$$

Taking the ratio of Eq. (1) to Eq. (2) above, we get Eq. (3)

$$\frac{r_p}{r_s} = \frac{\sin^2\theta - \cos\theta\sqrt{n_2^2 - \sin^2\theta}}{\sin^2\theta + \cos\theta\sqrt{n_2^2 - \sin^2\theta}} \quad \cdots (3)$$

By transforming Eq. (3) into an expression for n, we can obtain the complex permittivity by Eq. (4)

$$n_2^2 = \sin^2\theta + \frac{\sin^4\theta}{\cos^2\theta}\left(\frac{1-\frac{r_p}{r_s}}{1+\frac{r_p}{r_s}}\right)^2 = \varepsilon_1 - i\varepsilon_2 \quad \cdots (4)$$

ε_1: dielectric constant ε_2: absorption coefficient

III. Evaluation of Complex Permittivity by THz-TDS

Figure 3 shows the time waveform of the THz-TDS pulse signal that was reflected by metal with an incident angle of 60°. The peak amplitude of the S-wave is from -0.272 to +0.188 V, whereas the peak amplitude of the P-wave is from -0.234 to +0.176 V. The half pulse width was 0.3 psec.

Figure 4 shows the results of the Fourier transform of the time waveform shown in Fig. 3. The spectrum was unstable in the frequency range of below 200 GHz, and the intensity of the spectrum reached its maximum at about 300 GHz. In addition, it was found that the spectrum decreased at around 550 GHz and 750 GHz due to the absorption by atmosphere.

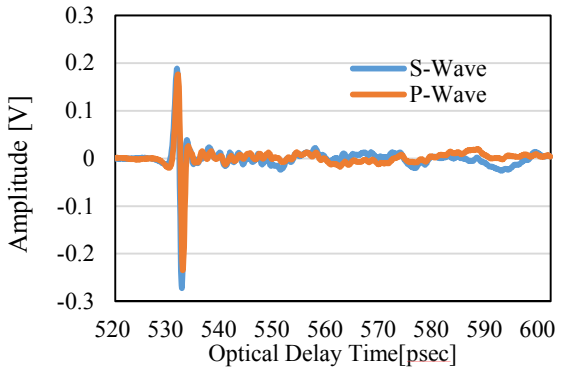

Fig. 3 Time waveform of the THz-TDS pulse signal that was reflected by metal with an incident angle of 60°.

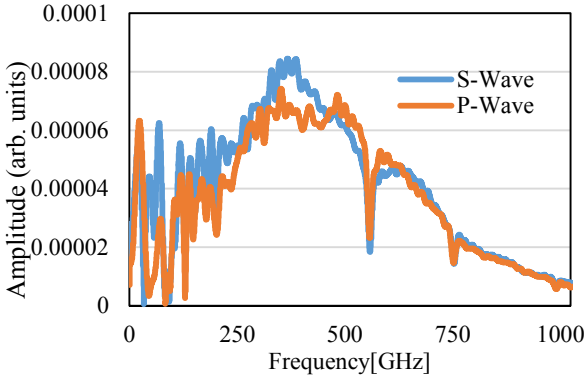

Fig. 4 Fourier transform of the time waveform shown in Fig. 3.

Figure 5 shows the pulse waveform reflected by a plastic with a thickness of 2 mm. In the original waveform, we can see the surface reflection at 530 psec and the backside reflection at 550 psec. The waveform of the surface reflection shows a waveform that rises and then falls, while that of the backside reflection shows a waveform that falls and then rises, indicating a phase shift of 180°. Complex permittivity calculation using Eq. (4) only considers the reflection at the sample surface, and the effect of backside reflection is not concluded. In order to eliminate the effects of backside reflection, we conducted time gating to the pulse waveform. As shown in Fig. 5, we replaced the pulse waveform intensity after 536 psec with 0.

Figure 6 shows the real part of the complex permittivity of the plastic calculated from the original waveform and the time-gated waveform shown in Fig. 5. In case we used the original pulse waveform for the calculation of complex permittivity, the real part of the complex permittivity fluctuated greatly depending on the frequency. If we calculate the complex permittivity using the time-gated pulse waveform, the real part of the complex permittivity shows almost constant value at all frequencies. These results indicate that eliminating the effects of multiple reflections by time-gating of the pulse waveform enables accurate calculation of complex permittivity of the sample.

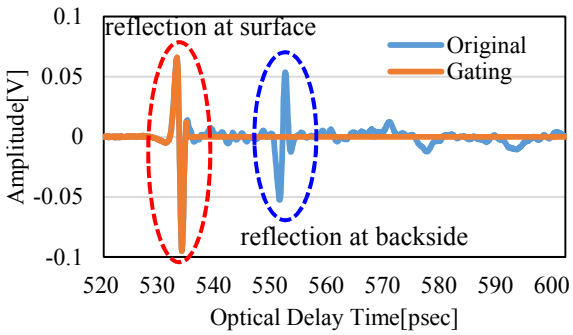

Fig. 5 The pulse waveform of a plastic sample.

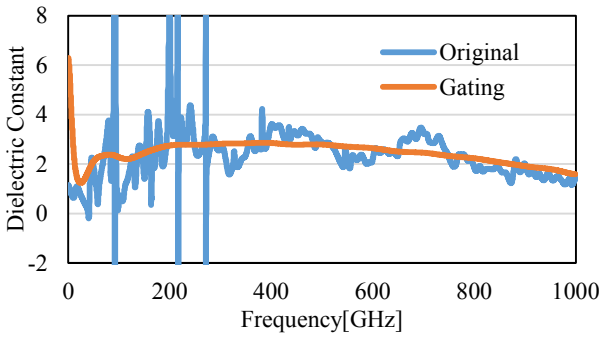

Fig. 6 Real part of plastic complex permittivity calculated from the pulse waveform with and without time-gating

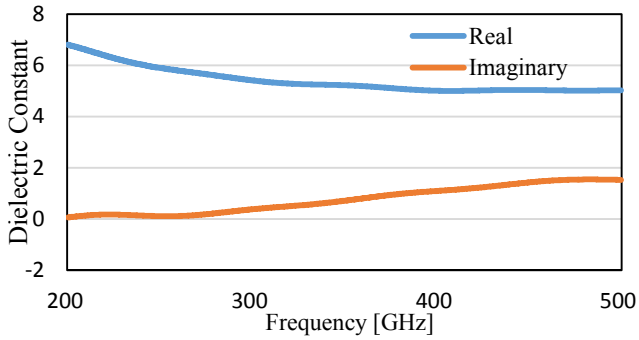

Fig. 7 Complex permittivity of concrete.

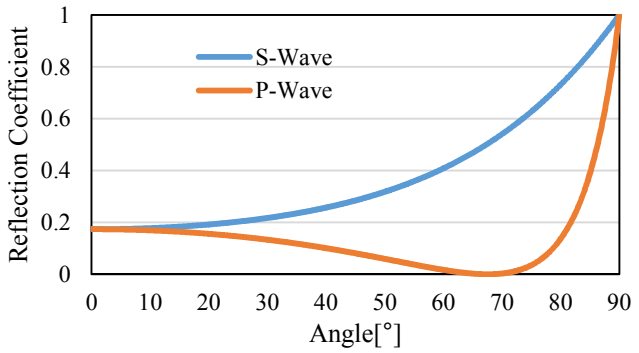

Fig. 8 Reflection coefficient of concrete

We calculated the complex permittivity of concrete, glass, and granite, from the time-gated pulse waveform. Figure 7 shows the calculated complex permittivity of the concrete using the pulse waveform measured by THz-TDS with the same method. At from 200 to 300 GHz, the real part of the concrete decreases significantly from 6.7 to 5.4. The real part of the complex permittivity became 5.4 to 5.0 at over 300 GHz, and the fluctuation became smaller than that at below 300 GHz. Imaginary part increases with frequency, and it was close to 0 at from 200 GHz to 270 GHz, and it gradually increased at from 270 to 470 GHz, and the imaginary part exceeded 1.0 after 400 GHz.

Figure 8 shows the angular dependence of the reflection characteristics of the concrete at 300 GHz, which was calculated from the complex permittivity of the concrete shown in Fig. 7. The reflection characteristics of the concrete was calculated using Eq. (1) and (2). The reflection coefficient of the s-polarized wave and p-polarized wave at 300 GHz is about 0.17 at 0°. The reflection coefficient of the s-polarized wave increases as the incident angle increases, while the reflection coefficient of the p-polarized wave becomes 0 at around 67° and then increases rapidly. At the incident angle of 67°, the numerator of Eq. (2) becomes zero, and this incident angle is called the Brewster angle.

We also evaluated the complex permittivity of the glass and granite in Fig. 9 and Fig. 10, respectively. In case of glass, the real part of the permittivity decreases from 7.3 to 6.3 at 200-500 GHz, and the imaginary part of the glass is found to be below 0.1 at 200-500 GHz. As for the real part of the granite, the value of the real part fluctuated between 5.4 and 6.2, and the imaginary part of the glass is below 0.1 at 200-500 GHz.

Table 1 summarizes the measured complex permittivity of the building materials. The complex permittivity at 95.9 GHz described in the Recommendation ITU-R is also described [4]. In case of the concrete, the real part was 0.78 smaller than that of ITU-R model and the imaginary part was almost the same as the ITU-R model. For the glass, both the real and imaginary parts are close to the ITU-R model. These results indicate that difference of the complex permittivity was below 1.0 for all of the building materials, and the ITU-R material property models at 95.9 GHz are roughly consistent with our experimental results at 300 GHz.

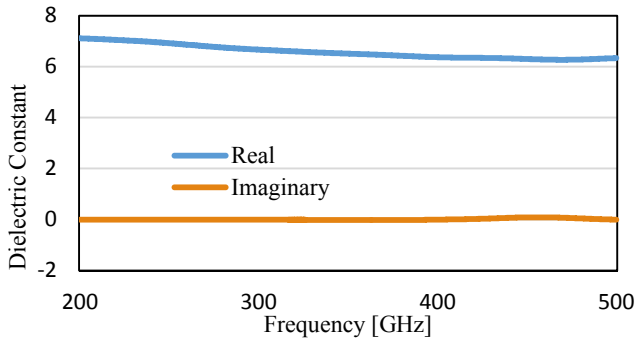

Fig. 9 Complex permittivity of the glass.

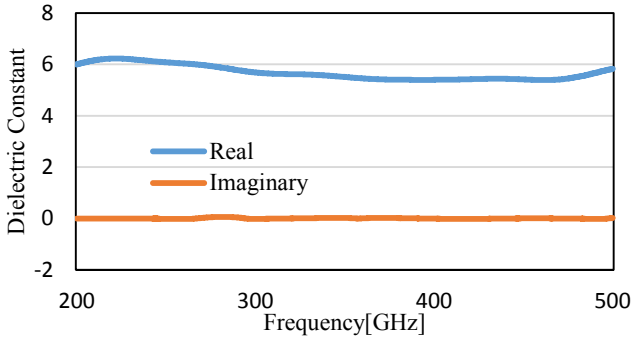

Fig. 10 Complex permittivity of the granite

Table. 1 Complex permittivity of the building materials.

	Our Model (@300GHz)	ITU-R Model (@95.9GHz)
Concrete	5.42 – j0.38	6.20 – j0.34
Glass	6.67 – j0.008	6.76 – j0.19
Granite	5.69 – j0.02	

IV. INDOOR RADIO PROPAGATION SIMULATION

We conducted indoor radio wave propagation simulations using the calculated complex permittivity of concrete and glass at 300 GHz and compared the simulation results that employs ITU-R material property models. The size of the room is 20 m x 60 m x 3 m. The height of Tx and Rx is 2 m, and omni-directional antenna with an E-plane half power beam width of 10° are used for Tx and Rx. The carrier frequency is 300 GHz and Tx output power is 10 dBm. The walls of the room are set to be concrete, and we set a glass (40 m x 1 m) that employs our material property model on the wall.

Figure 11 and Fig. 12 shows the simulation results of received power map that employs our material property model and ITU-R material property model, respectively. There is little difference of received power map around the transmitter. However, compared with the ITU-R model, the received power of our model is higher in many areas at the left side of the room. These results indicate that the reflection at high incident angle in our model is larger than that of ITU-R model.

V. CONCLUSION

We employed terahertz time-domain spectroscopy (THz-TDS) spectroscopy to obtain the complex permittivity of building materials, glass, concrete, and granite at 200-500 GHz. The use of fs pulse as a probe signal enables the effects of multiple reflection at the backside of the sample. The complex permittivity of concrete, glass, and granite was calculated from the time-gated reflected pulse signals, and the measured complex permittivity at 300 GHz was roughly matched with the ITU-R models at 95.9 GHz.

We conducted indoor radio wave propagation simulations using the measured complex permittivity of concrete and glass at 300 GHz. The simulation results indicate that that the reflection at high incident angle in our model is larger than that of ITU-R model.

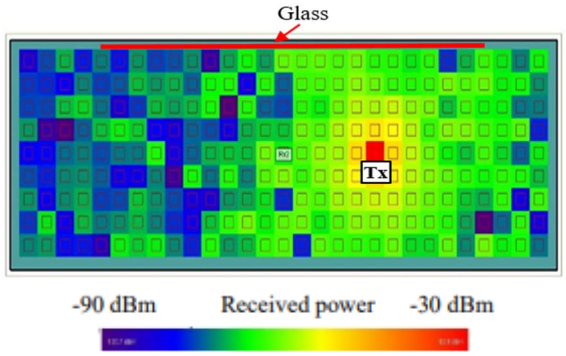

Fig. 11 Simulation results of received power map that employs our material property models.

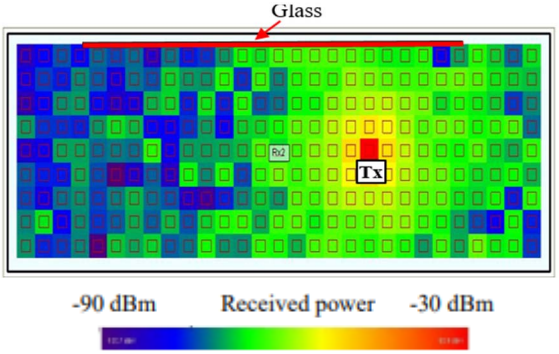

Fig. 12 Simulation results of received power map that employs ITU-R material property models [5].

ACKNOWLEDGMENT

This work was partly supported by the Japan-Europe Joint Program of the National Institute of Information and Communications Technology (NICT), and JSPS Grants-in-Aid for Scientific Research (A) Grant Number JP18H03827.

REFERENCES

[1] J-B. Doré, D. Belot, E. Mercier, S. Bicaïs, G. Gougeon, Y. Corre, B. Miscopein, D. Kténas, E. Calvanese Strinati, "Technology Roadmap for Beyond 5G Wireless Connectivity in D-band", 2020

[2] T. Nagashima, M. Hangyo, "Deve;opment of Terahertz Ellipsometry and Its Application to Evaluation of Semiconductors",Osaka University.2002

[3] S. Kawabata,"Fundamentals and Application of Ellipsometry",Tokyo Polytechnic University,2014

[4] "Propagation data and prediction methods for the planning of indoor radiocommunication systems and radio local area networks in the frequency range 900 MHz to 100 GHz", Recommendation ITU-R P.1238-7.2012 .

[5] "Propagation data and prediction methods for the planning of indoor radiocommunication systems and radio local area networks in the frequency range 300 MHz to 100 GHz", Recommendation ITU-R P.1238-9.2017